Zone-Fingerprinting: Unlocking the Power of Fingerprinting for Indoor Localization in 5G

Antonin Le Floch
Alsatis, Université de Toulouse, CNRS, Toulouse INP, UT3
Toulouse, France
antonin.lefloch@irit.fr

Rahim Kacimi
Université de Toulouse, CNRS, Toulouse INP, UT3
Toulouse, France
rahim.kacimi@irit.fr

Pierre Druart
Alsatis
Toulouse, France
pierre.druart@alsatis.com

Yoann Lefebvre
Alsatis
Toulouse, France
yoann.lefebvre@alsatis.com

André-Luc Beylot
Université de Toulouse, CNRS, Toulouse INP, UT3
Toulouse, France
andre-luc.beylot@irit.fr

***Abstract*—Indoor localization is either achieved through dedicated radio networks or opportunistically by leveraging existing networks. The preferred method is to compare the received signal strength (RSSI) with a reference map, commonly known as Fingerprinting. However, as network operators often space out radios to minimize costs and maximize spectral efficiency, large areas exist where the radio pattern remains similar, leading to significant inaccuracies in Fingerprinting results. To address this issue, we propose changing the paradigm by not predicting a single point with an uncertainty area, but rather the exact zone where the user is located. To further refine the positioning of the user within this zone, we integrate the Zone-Fingerprinting technique with pedestrian dead reckoning, enabling us to determine the specific subpart of the zone where the user is located. Our goal is to locate at-risk workers in hospitals, and to achieve this, experiments were conducted in both a hospital environment and an office environment, utilizing a 5G private network. The results indicate that Zone-Fingerprinting is more reliable than traditional Fingerprinting.**

***Index Terms*—5G, Indoor Localization, Zone-Fingerprinting, Pedestrian Dead Reckoning, Experimentations**

I. Introduction

While outdoor localization is addressed by GPS and RTK offering decimeter accuracy [1], the same is not true for indoor environments where these signals are absent. Nevertheless, developing an indoor localization service is crucial for navigation, locating objects, or assisting individuals in emergencies. In this paper, we specifically address the challenge of locating at-risk workers inside hospitals and office environments. Two main approaches exist for indoor localization: dedicated solutions, which are costly but highly precise [2], and opportunistic solutions, which leverage existing radio networks but must contend with their inherent limitations.

In this field, the preferred approach for ubiquitous localization relies on comparing signal measurements to a reference map, a method commonly referred to as fingerprinting [3]. The precision in this approach is derived from the diversity of received signals, as it cannot distinguish between areas with identical signal. However, these uncertainty zones are far from rare as wireless network deployments optimize for coverage and spectral efficiency, minimizing the number of antennas and overlapping zones.

ISBN 978-3-903176-72-0 © 2025 IFIP

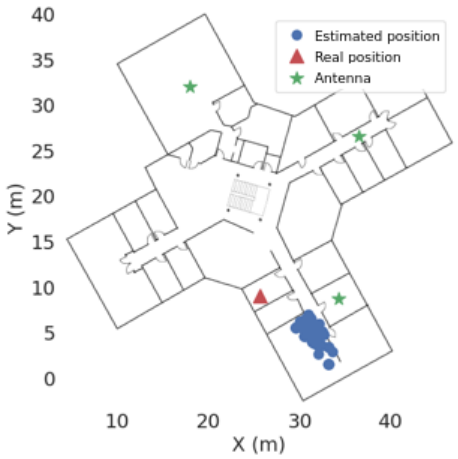

Fig. 1. Estimated position of a user located at the red triangle over five minutes, using classical fingerprinting.

For instance, Figure 1 illustrates how fingerprinting estimates a position at the center of a zone where only a single cell is reachable. This is due to numerous positions sharing the same received power, as illustrated by Figure 2. To minimize the mean error, the fingerprinting algorithm predicts a position at the center of this area. To address this lack of spatial resolution, some [4] propose to add gateways, thus increasing the overall cost while degrading radio performances.

In contrast, we propose leveraging these zones not to predict an uncertain position but to determine an exact area shown in Figure 2. However, it can be sparse and large. To refine the localization, we divide it into clusters to identify the one closest to the actual position, as illustrated by Figure 3. However, since these clusters are equiprobable by design, signal power alone is insufficient to distinguish between them.

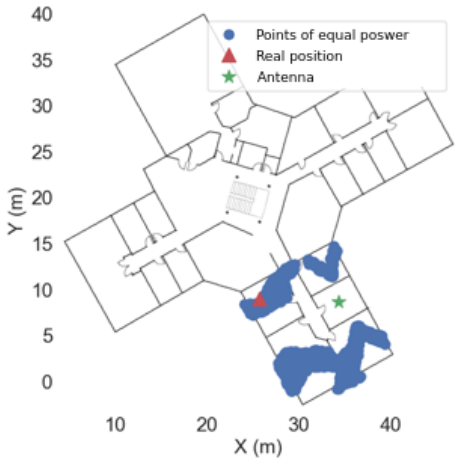

Fig. 2. All points sharing the same received power as the user located in the red triangle.

To overcome this limitation, we integrate another localization method known as Pedestrian Dead Reckoning (PDR). This incremental approach utilizes accelerometer and magnetometer measurements to estimate the path followed by a moving user. When the user reaches a location, the most probable cluster is determined as the one closest to the arrival position. A weight is also assigned to each cluster, as defined in (1) and (2), where d_i represents the Euclidean distance between the arrival position and the centroid of the i^{th} cluster. These weights are illustrated in Figure 3.

$$w_i = \frac{1}{d_i \cdot C} \tag{1}$$

$$C = \sum_{i=0}^{n} \frac{1}{d_i} \tag{2}$$

Beyond predicting the exact zone containing the user, we also propose identifying the cluster most likely to contain the actual position.

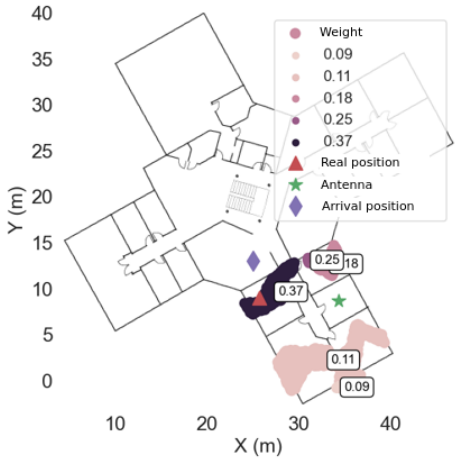

Fig. 3. Zone-Fingerprinting Paradigm. Cluster's weights depends on the distance to the arrival position predicted by PDR.

The remainder of this paper is organized as follows. In Section II, we survey related work. Section III introduce our 5G experimental setup designed to represent typical private indoor networks. Section IV contains the core of the paper, where we present Zone-Fingerprinting. The Section V provide insight on our clustering approach. We then explain in Section VI how Zone-Fingerprinting combined with PDR can rank the clusters by importance. Our algorithm is then experimentally tested in Section VII and compared to state-of-the-art methods. Finally, in Section VIII we discuss our work and present our conclusions in Section IX.

II. Related work

Since the development of the RADAR system in 2000 [3], fingerprinting has achieved considerable success, particularly in Wi-Fi [5]. Current research directions [6] focus on algorithmic improvements through deep learning [7] or diverse applications of Channel State Information (CSI) [8].

On the over hand, dead reckoning has being used since antiquity to navigate overseas. Its application in smartphones relies on the Inertial Measurement Units (IMUs) and is based on a starting point determined with GPS [9] or an RFID gate [10]. Current research focus on machine learning to infer the stride length either by regression [11] or classification [9].

As the current goal for indoor localization is precision, research lacks zone-based localization, as emphasized by its absence in surveys [6]. Nevertheless, some have suggested area predictions linked to fingerprinting. These approaches generally involve clustering a building to predict predefined areas such as a room or corridor [12]–[15]. This manual method becomes cumbersome for large buildings, leading Laska et al. [16] to propose an automated way to generate these zones. However, they share the same bias of considering each room having a unique radio signature.

To differentiate zones sharing the same electromagnetic power, it may be possible to consider additional measurements to resolve ambiguities. An approach could involve leveraging the Reference Signal Received Quality (RSRQ), the time of flight, or the CSI. However, the RSRQ is not predictable, as it depends on the radio context [8]. Measuring the time is a challenging approach, requiring precise measurements through dedicated firmware. Currently, the Timing Advance (TA) can be used in 5G, but its granularity in our network is $2.6 \cdot 10^{-7}s$ or 39 meters [17]. The CSI is very promising towards achieving precise localization [18] but requires complete signal analysis through dedicated firmware and Software Defined Radio (SDR).

III. Experimental setup and 5G

Technologies capable of supporting a ubiquitous indoor localization method include Wi-Fi [5] and 5G [19]. The latter, in particular, has greatly standardized localization since Release 16 [20]. Its unique characteristics in terms of throughput and latency are of significant interest to the industry, which also requires an indoor localization service to improve processes or locate production tools. The Zone-fingerprinting algorithm is thus tested in a private 5G network for industrial applications.

The following describe the experimental setup used. A full 5G network has being deployed at our building and is composed of Amarisoft Next Generation NodeB (gNB), AW2S panther Remote Radio Head (RRH), and Halys Core Network (CN), thus representing a realistic 5G private network. The rest of our equipments are shown in Figure 4.

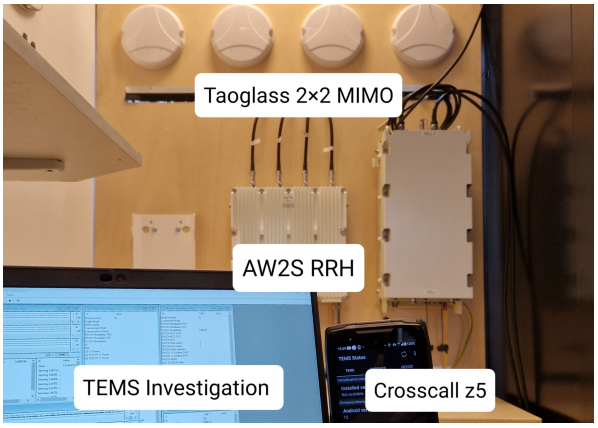

Fig. 4. AW2S RRH, Taoglass radio, TEMS software and Crosscall-Z5 smartphone in the Alsatis lab.

Radio are distributed all around the building, with three cells on the first floor and two on the second floor. Finally, the radio details are presented in Table I.

TABLE I
RADIO PARAMETERS

Radio parameters on Amarisoft gNB				
Band	*Mode*	*Subcarrier Spacing*	*Bandwidth*	*Frequency*
n77	TDD	30 kHz	100 Mhz	3.9–4.0 GHz

Radio parameters were validated using radio tools.

Our decision to utilize a 5G network stems directly from its application in industrial environments with high demands for connectivity and localization. Since Release 16 [20], the 3GPP has specifically defined functions and protocols dedicated to localization (Figure 5). Of the two dedicated protocols, only the NR Positioning Protocol A (NRPPa) is supported by network equipment manufacturers. We therefore use it to directly collect power measurements within the network core through RRC reconfiguration requests sent by the gNB. However, the control plane traffic generated by these measurement requests for localization significantly increasing the load on the AMF, which must also be modified to support these use cases.

IV. ZONE-FINGERPRINTING

A. *Fingerprinting in a nutshell*

As illustrated by Figure 8, fingerprint can be divided into two parts; an offline phase consisting in creating a reference map and the training of machine learning models, and an online phase where the signal is collected, cleaned and fed into the models to predict the position in real time. For scalability and precision, we have generated the reference map using a previously developed tool named ORPELA

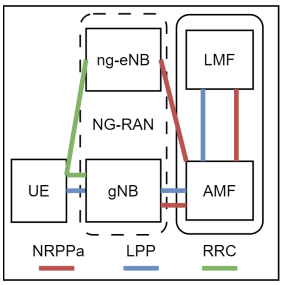

Fig. 5. 5G protocols designed for localization.

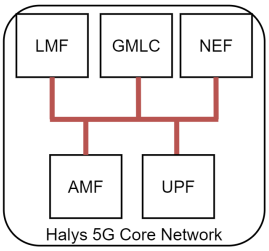

Fig. 6. 5G Core network functions dedicated to localization.

[19], [21]. This method involves creating a 3D model of the building using the 3D modeling software Blender, as illustrated in Figure 7. In this model, light sources represent radio signals, and walls are modeled as semi-transparent materials. By leveraging the built-in advanced light modeling system with path tracing, light intensity can be assimilated to radio power. With only a very limited number of calibration points (six in total), a complete reference power map of the building can be generated. Finally, this method achieves accuracy comparable to state-of-the-art software like Atoll.

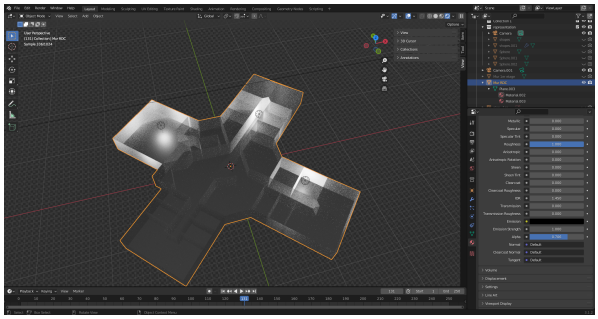

Fig. 7. A view of the Alsatis building inside Blender. With ORPELA, the radio are represented by light sources and wall are semi-transparent material.

Regarding the machine learning, a two-model approach is used, the first being a classification model predicting the floor and the second a regression model predicting a position at a given floor. The nature of these models is derived by the data to be predicted, respectively discreet and continuous. During the online phase, the signal is first measured then cleaned by averaging it over ten seconds to minimize the power variance. This estimator denoted P is then used to as an input to both models in order to predict a floor and a position.

The reference map is summarized in Table II. Each reference point $r = (x, y, z)$ is associated with the expected received power P. For cells that are out of range, a power level of $-135db$, representing the lower limit in this context, is assigned.

The models are subsequently trained on this reference map to predict a position based on a given measurement. This approach relies on the assumption that each position corresponds uniquely to a specific measured power. However, if multiple regions exhibit identical electromagnetic power levels, distinguishing between them using this criterion alone becomes impossible.

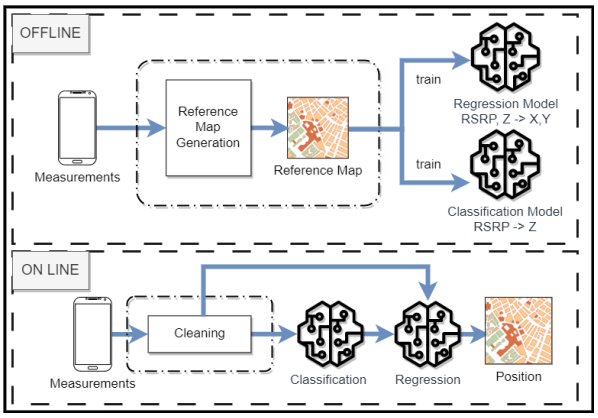

Fig. 8. Fingerprinting in a nutshell.

TABLE II
FINGERPRINTING

Reference Map Representation			
Position	Cell 1	Cell 2	Cell 3
(x1,y1,z1)	-135 dB	-135 dB	-89 dB
(x1,y2,z1)	-135 dB	-75 dB	-135 dB
(x2,y1,z2)	-100 dB	-135 dB	-135 dB
...	...	...	...

B. Zone-Fingerprinting principle

To modify the behavior of the models, we adjusted the reference map to associate a given power P with a zone $\Omega = [r_1, r_2 ... r_N]$ instead of a single point $r = (x, y, z)$. This zone corresponds to all points within a power range of $P \pm \epsilon$ as illustrated by Table III. To construct this new reference map, an algorithm identifies all neighboring points within an ϵ-radius of each position listed in Table II.

TABLE III
ZONE-FINGERPRINTING

New Reference Map Representation			
List of similar points	Cell 1	Cell 2	Cell 3
(x1,y1,z1), (x1,y5,z1), (x11,y8,z1) ...	-135 dB	-135 dB	-89 dB
(x1,y2,z1), (x4,y10,z1), (x3,y9,z1) ...	-135 dB	-75 dB	-135 dB
(x2,y1,z1), (x6,y6,z1), (x6,y2,z1) ...	-100 dB	-135 dB	-135 dB
...	...	...	...

C. On how to size the area

Our new model predicts the zone in which the user is located. The size of this area is a crucial parameter in zone-fingerprinting. A value of ϵ that is too small will produce a zone that does not include the actual position, whereas a value that is too large will yield a zone too large to be useful in localization. The aim is therefore to find a value of ϵ that ensures the presence of the user in the zone, while minimizing the surface area. Equation (3) quantifies how well a real position fits within the predicted zone Ω, while Equation (4) evaluates the percentage of successful predictions over a set of N tested values.

$$\mathcal{A}(r, \Omega) = \begin{cases} 1 \text{ if } r \in \mathring{\Omega} \\ 0 \text{ else} \end{cases} \tag{3}$$

where $\mathring{\Omega}$ is the interior of Ω.

$$\xi = \frac{1}{N} \sum_i \mathcal{A}(r^i, \Omega^i) \tag{4}$$

Several ϵ values were tested to generate multiple reference maps, and models were trained on these maps. Sixteen measurements, each lasting five minutes, were conducted throughout the building, as shown in Figure 12. These served as an input to estimate a zone using Zone-Fingerprinting. For each area, ξ and the average surface is computed. The results, presented in Figure 9, guided our decision to select $\epsilon = 3$. This choice is particularly relevant, as it is correlated to the variance of the estimator P, which averages at $3dB$.

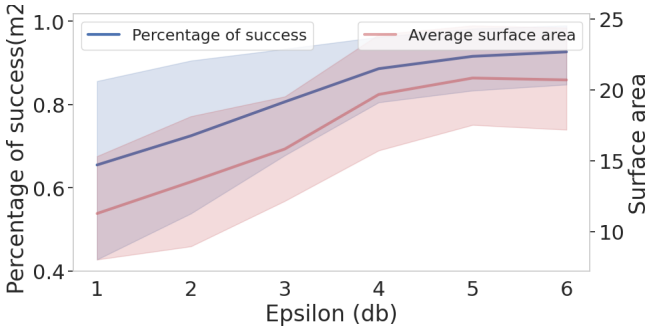

Fig. 9. Percentage of success and average area relative to ϵ.

D. Is a machine learning model necessary?

The goal of the machine learning model is to identify all points that are similar from a radio perspective. But why not simply retrieve this list directly from a database? The key difference between these approaches lies in their execution times. We measured the time required to predict the zone for 500 different power values. For each point, the model takes approximately $\sim 3.1 \cdot 10^{-5} s$, while the database search takes around $\sim 2.5 \cdot 10^{-3} s$, making the database approach roughly a hundred times slower.

V. CLUSTERING ZONES FOR PRECISE LOCALIZATION

The estimated zone can be large, making it time-consuming to locate an object within it. To address this, we propose partitioning the zone into a set of sub-zones, commonly referred to as clusters. The aim is to identify the cluster closest to the real position. The entire predicted zone Ω can be subdivided into k clusters, as defined in Equation (5). This step is performed using the density-based clustering algorithm named DBSCAN.

$$\begin{gathered} \Omega = \{\omega_1, \omega_2, \omega_3, \cdots, \omega_k\}, \\ \text{avec } \omega_i \neq \emptyset, i = 1, \cdots, k \end{gathered} \tag{5}$$

DBSCAN works by grouping points labeled as ”dense” to form clusters. To classify a point as ”dense,” DBSCAN relies on a maximum distance d to define neighboring points

and a minimum number of neighbors $MinPts$ required for a point to be considered part of a dense region. Given that the reference map has a granularity of one point every $10cm$, we set $d = 20cm$. The maximum number of points within a $20cm$ radius is 12, we thus choose $MinPts = 6$. Other values were tested but produced less accurate results than the one reported in Section VII.

VI. Fingerprinting for Indoor RSRP Areas (FIRA)

To address the challenge of ranking the clusters, we propose leveraging another localization method based on pedometer and magnetometer measurements from smartphones, commonly known as PDR.

A. Dead reckoning in a nutshell

PDR navigation relies on measuring the distance d_t and direction θ_t from a known position (x_0, y_0) (6). While it has been used since ancient times for maritime navigation, modern applications leverage the IMUs found in every smartphone. Distance measurements are performed using the pedometer, accelerometer, and gyroscope, while direction is determined through the gyroscope and magnetometer.

$$\begin{aligned} x_n &= x_0 + \sum_{t=1}^{n-1} d_t \cdot \cos(\theta_t) \\ y_n &= y_0 + \sum_{t=1}^{n-1} d_t \cdot \sin(\theta_t) \end{aligned} \tag{6}$$

1) Distance: The distance can be calculated by integrating the accelerometer data over time. However, this method proves to be inaccurate due to a slight bias present in each measurement. A better approach is to use the accelerometer to determine the number of steps taken and then multiply this by a stride length, as shown in (1).

$$d_t = N_{step} \cdot L_{step} \tag{7}$$

N_{step} is typically obtained with pedometer measurements. Four different smartphones are benchmarked to evaluate their pedometer quality. The evaluation consisted of walking fifty steps with a smartphone in a pocket, moving in a random pattern. A total of ten repetitions were performed, and the results are shown in Figure 10. We can observe that, except for the "Xiaomi" phone, all three other smartphones are quite close to the real number of steps.

Estimating L_{step} is a much more challenging task, as this value varies from one individual to another and can change while walking. Therefore, we chose to draw from the work of Hannink et al. [11] and selected the value corresponding to the morphology of the person conducting the tests, which is a stride length of $80cm$.

2) Direction: The direction is estimated using the gyroscope and the magnetometer. The gyroscope provides insights into the position of the smartphone inside a pocket (whether it is up or down), while the magnetometer indicates the orientation relative to the Earth's magnetic field. Combining both measurements gives the orientation of the user in space. The main challenge lies in the imprecision of the magnetometer measurements. Extensive experiments conducted by Rai et al. [22] revealed an error of 15 degrees for 90% of building surfaces. This value can be used to estimate the overall imprecision of PDR overtime.

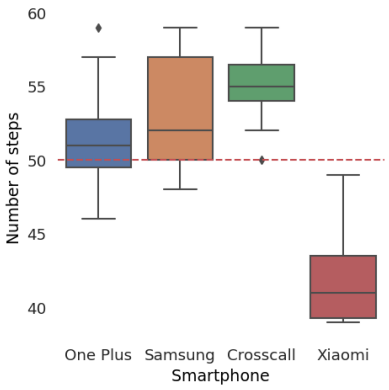

Fig. 10. Pedometer values estimated by four smartphones.

B. PDR evaluation

Four different phones are used to evaluate PDR performances, as shown in Figure 11.

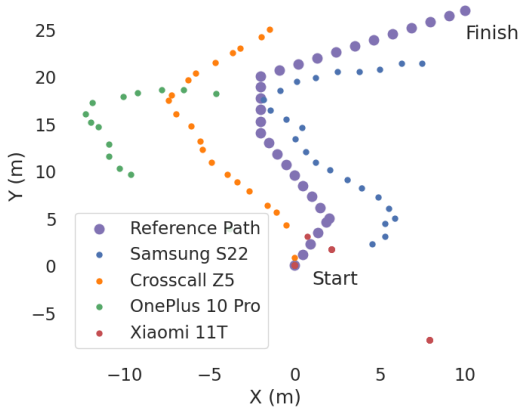

Fig. 11. Pedometer values estimated by four smartphones.

While the overall reference path is well predicted by the Crosscall and Samsung devices, the One Plus and Xiaomi perform poorly due to a lack of measurements returned to the Android application by the firmware. The One Plus takes a long time to report the first value, while the Xiaomi only provides a new value every $10s$.

Overall, two main limitations should be underlined. First, PDR requires a starting point, as it is an iterative method. Second, it requires frequent calibrations, as small errors accumulate over time.

C. Fusion between fingerprinting and PDR

Some previous studies have already proposed merging fingerprinting with PDR [23], using the former when the user is static and the latter when the user is in motion. This combined approach named PDR and RSRP Interplay

for Localization Using 5G Networks (PRILUN) significantly improves the precision during movements.

Our new algorithm essentially builds on what was previously introduced. If the user is stationary, fingerprinting is used; if the user is in motion, their distance is estimated using PDR navigation. The key difference here is that the position predicted by fingerprinting is not unique, whereas a starting point for the PDR must be defined. To address this, we propose clustering the predicted zones and identifying the centroid closest to the arrival position determined by PDR. This cluster's centroid will then serve as a new starting point for the PDR algorithm. FIRA is detailed in Algorithm 1, and its key features are presented below.

Algorithm 1 Pseudocode of FIRA

```
while Localization is ongoing do
    Retrieve data: Reference Signal Received Power (RSRP), Pedometer, Magnetometer
    Process data:
    Zone ← Model prediction (RSRP)
    (d, θ) ← Transformation (Pedometer, Magnetometer)
    if The user is stationary then
        Cluster the Zone and assign Weights based on the arrival point
        Current Position ← Zone
    else The user is moving
        if The user just started moving then
            if First movement then
                Initialize the system (Section VI-C2)
            end if
        end if
        Current Position ← Calculate position using PDR (d, θ)
    end if
    Wait one second
end while
```

1) Arrival at a Location: When a user arrives at a new location, a switch is made from PDR navigation to Zone-Fingerprinting. To work with power values consistent with the current position, the system is paused for five seconds. This value corresponds to half the sliding window used to average the signal (Section IV-A). After this delay, the measured power is used to predict a zone that is then cluster using DBSCAN. The distance between each centroid to the arrival point is then computed to give weight according to (1) and (2).

2) Initialization: Initialization is the most complex part of the process. How can the starting point for PDR navigation be determined from a zone? Upon device activation, the system waits for the first instance where the user is stationary to determine an initial zone. At this stage, it is impossible to precisely locate the user within this zone. To determine the starting point, we wait for the user to move to another zone and retroactively estimate the most probable starting cluster. If the system encounters a particular scenario preventing convergence to the correct solution, all the closest arrival zones will be considered equally probable. The process will then be repeated until a unique solution is found. Once the starting position is estimated, the rest of the algorithm can proceed.

VII. Experimentations

A. How to compare to Fingerprinting?

Estimating the Fingerprinting error is a straightforward task, as it involves calculating the distance between the actual position and the estimated one. In contrast, calculating the distance between a zone and a point is not as simple. Indeed, one can consider either the average distance (8) or the minimum distance (9). The average distance significantly underestimates the accuracy of our system, whereas the minimum distance provides a lower bound on the error.

$$\mathcal{D}_{mean} = \frac{1}{k} \sum_{\widehat{r}_i \in \Omega} \| r - \widehat{r}_i \| \quad \text{Where } k \text{ is the cardinal of } \Omega \tag{8}$$

$$\mathcal{D}_{min} = \min_{\widehat{r}_k \in \Omega} (\| r - \widehat{r}_k \|) \quad \text{Where } \widehat{r}_k \text{ the centroid of the cluster } \omega^k \tag{9}$$

A more accurate metric is to consider the distance between the centroid of the cluster with the greatest weight, as shown in (10). Indeed, this cluster is, by construction, the most probable to contain the real position and will be the first one to be explored when searching for a tool or an at-risk worker.

$$\mathcal{D}_{cluster} = \| \mathfrak{C} - \widehat{r}_k \| \quad \text{Where } \mathfrak{C} \text{ is the centroid of the cluster with the greatest weight.} \tag{10}$$

B. Zone-Fingerprinting performances

To compare these metrics with classical Fingerprinting, a total of sixteen measurements were conducted in a building, each lasting five minutes. The cumulative distribution function (CDF) of the error for each metric is presented in Figure 13. A clear gain can be observed when comparing the distance from the best cluster to conventional Fingerprinting.

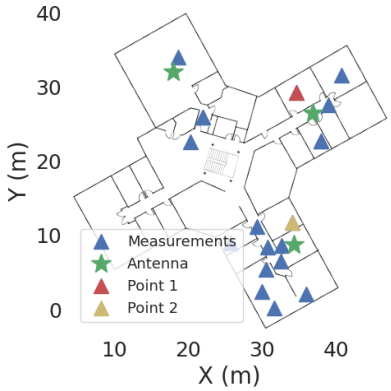

Fig. 12. Measurement points.

To better observe the behavior of our system, we plotted the error over time for two points in Figures 14 and 15. These

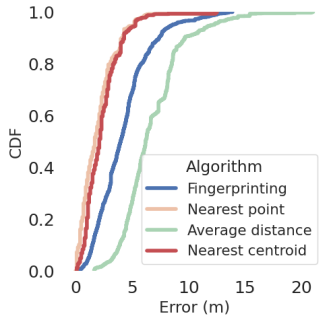

Fig. 13. Cumulative Distribution Function of the error for each metric.

plots highlight the similarity between classical Fingerprinting and the average distance to the predicted zone. Furthermore, the error variance is relatively low, particularly in comparison with traditional Fingerprinting estimates. This is because our system predicts a zone rather than a single point, making it less sensitive to power variations.

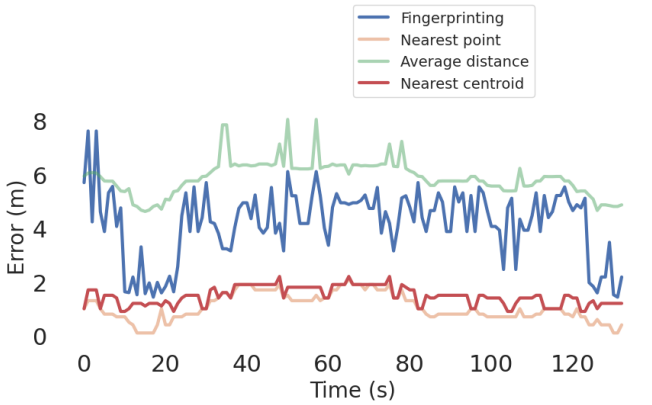

Fig. 14. Error as a function of time on point 1.

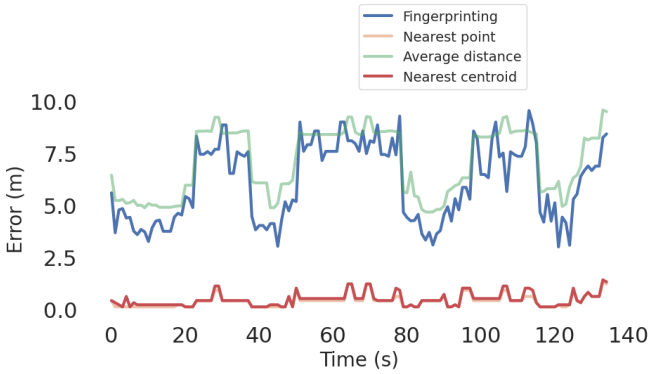

Fig. 15. Error as a function of time on point 2.

C. FIRA performances

Ten experiments were conducted to evaluate FIRA, with a moving user following the path represented in Figure 16. As a reference from the literature, the algorithm PRILUN (Section VI-C), used to combine PDR and the classical Fingerprinting, is represented in Figure 17. Finally, Figure 18 depicts the trajectory predicted by FIRA, along with the weights. Three key observations can be drawn from this graph.

1) General Overview: First, our algorithm achieves good overall accuracy, both during static phases and user movements. Moreover, the search areas remain relatively narrow. Even if the user is not in the cluster with the greatest weight, they can iteratively move to other possible positions. Such information is absent in classical Fingerprinting and provides valuable insights for a rescue team searching for an injured worker.

2) Static Points: The final estimated zone is the most precise, as it lies at the intersection of multiple cells and benefits from high spatial resolution. The "Pause" zone is larger, but still encompasses the actual position. Since this position is in direct line of sight and near an antenna, the algorithm naturally predicts a dense zone containing all nearby points. Finally, the "Starting" zone includes the real position, but the algorithm assigns an incorrect probability of presence. An explanation for this behavior is provided in the following.

3) Initial Path: The initial path highlights a particular feature of the algorithm. During the initialization phase, FIRA seeks to minimize the error at the arrival point. As a result, the initial movement accurately represents the path the user followed toward the "Pause" point. This approach comes at the expense of reduced accuracy at the starting point. However, it is impossible to determine the first point precisely. Therefore, our solution only correctly estimates the presence probability starting from the second static position.

It should also be noted that our approach provides a search area for the user. If the highest-probability location does not correspond exactly to the real position, the algorithm provides an exact search area.

D. Quantitative results

To better encompass the benefits from Zone-Fingerprinting, we plotted the error as a function of time in Figure 20. The error for the FIRA algorithm is computed based on the most probable position over time, described by (10) and illustrated in Figure 19. This method provides an imperfect estimation of the distance to a zone. However, we assume that a system user would rely on the cluster with the greatest weight.

1) Notes on the "Pause": The only significant difference between FIRA and PRILUN occurs when the user is at the "Pause" point. Observing Figure 18, we notice that FIRA predicts a zone centered on the antenna. Thus, the point used to plot Figure 19 is located directly under the antenna. On the other hand, traditional Fingerprinting provides a position closer to the user, except when the power briefly increases, leading the estimated position to also shift beneath the antenna. This discrepancy in precision is therefore attributable to the comparison method.

2) Overall Results: The CDF of the error, illustrated in Figure 21, shows that, on average, the cluster estimated by

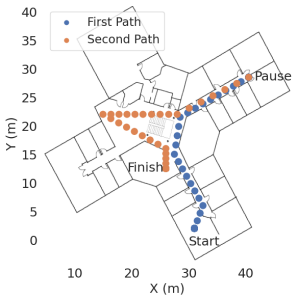

Fig. 16. Reference path.

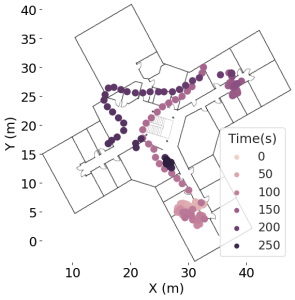

Fig. 17. Position estimation using PRILUN.

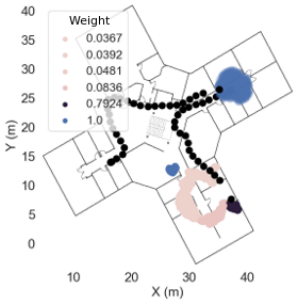

Fig. 18. Position estimation using FIRA.

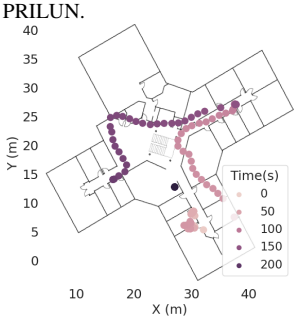

Fig. 19. Point used to calculate the error generated by FIRA as in (10).

FIRA is closer to the real position than the one estimated by PRILUN. It should also be noted that most of the points and trajectories originate from the initialization phase, which is the least precise part of the algorithm. As a result, Figure 21 somewhat underrepresents the actual performance of FIRA.

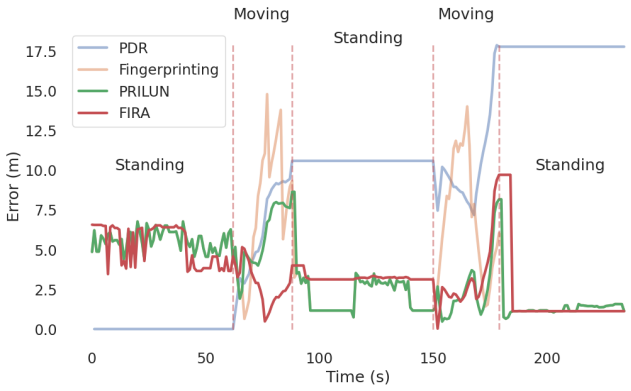

Fig. 20. Error as a function of time for each method.

VIII. Discussion

In this part, we want to discuss the limits of our approach and the main challenges that need to be addressed.

Determining the cluster weights heavily relies on PDR. As the user moves for a long time, the precision of this method declines, and the predicted arrival point can no longer be used in isolation. Thus, it must be combined with an uncertainty estimation to improve the accuracy of the results.

A truly ubiquitous indoor localization system must contend with the topology of radio networks, which often lack the spatial diversity needed to differentiate areas. Additionally, it must be built on an automated system for generating reference maps. For instance, a path tracing based algorithm like ORPELA [19], [21] still requires manual configuration.

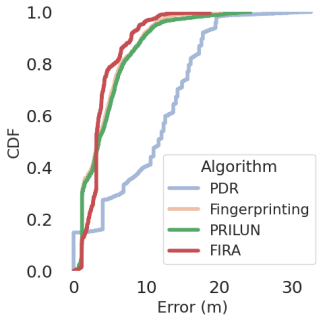

Fig. 21. CDF of the error for each method.

IX. Conclusion

In this paper, we present a new paradigm for indoor localization called Zone-Fingerprinting that leverages existing radio networks. Rather than predicting a point with an uncertainty radius, we estimate the exact zone where the user is located. Furthermore, we combine this method with PDR to rank clusters based on their probability of presence, providing crucial information about where to search for a tool or a worker-at-risk.

This algorithm is perfectly designed to address sparse radio environments, which represent the vast majority of existing networks. Our experiments in a 5G environment allowed us to benchmark its performance against other works in the literature, underlining its reliability.

A potential direct improvement could be to combine our approach with map-matching methods to improve the PDR. We are firmly convinced that the future of indoor localization will rely on integrating multiple methods.

References

[1] D. S. M. Valente, A. Momin, T. Grift, and A. Hansen, "Accuracy and precision evaluation of two low-cost RTK global navigation satellite systems," *Computers and Electronics in Agriculture*, vol. 168, p. 105142, Jan. 2020. [Online]. Available: https://www.sciencedirect.com/science/article/pii/S0168169918312602

[2] J. Schroeder, S. Galler, K. Kyamakya, and K. Jobmann, "Nlos detection algorithms for ultra-wideband localization," in *2007 4th Workshop on Positioning, Navigation and Communication*, 2007, pp. 159–166.

[3] P. Bahl and V. Padmanabhan, "RADAR: an in-building RF-based user location and tracking system," in *Proceedings IEEE INFOCOM 2000. Conference on Computer Communications. Nineteenth Annual Joint Conference of the IEEE Computer and Communications Societies (Cat. No.00CH37064)*, vol. 2, Mar. 2000, pp. 775–784 vol.2, iSSN: 0743-166X. [Online]. Available: https://ieeexplore.ieee.org/document/832252

[4] S. Djosic, I. Stojanovic, M. Jovanovic, T. Nikolic, and G. L. Djordjevic, "Fingerprinting-assisted uwb-based localization technique for complex indoor environments," *Expert Systems with Applications*, vol. 167, p. 114188, 2021. [Online]. Available: https://www.sciencedirect.com/science/article/pii/S0957417420309222

[5] S. He and S.-H. G. Chan, "Wi-fi fingerprint-based indoor positioning: Recent advances and comparisons," *IEEE Communications Surveys And Tutorials*, vol. 18, no. 1, pp. 466–490, 2016.

[6] G. Deak, K. Curran, and J. Condell, "A survey of active and passive indoor localisation systems," *Computer Communications*, vol. 35, no. 16, pp. 1939–1954, Sep. 2012. [Online]. Available: https://linkinghub.elsevier.com/retrieve/pii/S014036641200196X

[7] H. Meng, F. Yuan, T. Yan, and M. Zeng, "Indoor positioning of rbf neural network based on improved fast clustering algorithm combined with lm algorithm," *IEEE Access*, vol. 7, pp. 5932–5945, 2019.

[8] Z. Yang, Z. Zhou, and Y. Liu, "From rssi to csi: Indoor localization via channel response," *ACM Comput. Surv.*, vol. 46, no. 2, dec 2013. [Online]. Available: https://doi-org.gorgone.univ-toulouse.fr/10.1145/2543581.2543592

[9] J.-G. Krieg, G. Jakllari, H. Toma, and A.-L. Beylot, "Acrux: Indoor Localization Without Strings," in *Proceedings of the 20th ACM International Conference on Modelling, Analysis and Simulation of Wireless and Mobile Systems*. Miami Florida USA: ACM, Nov. 2017, pp. 187–196. [Online]. Available: https://dl.acm.org/doi/10.1145/3127540.3127545

[10] "Sysnav navigation technologies," accédé le : 25-07-2024. [Online]. Available: https://www.sysnav.fr/

[11] J. Hannink, T. Kautz, C. F. Pasluosta, J. Barth, S. Schülein, K.-G. Gaßmann, J. Klucken, and B. M. Eskofier, "Mobile stride length estimation with deep convolutional neural networks," *IEEE Journal of Biomedical and Health Informatics*, vol. 22, no. 2, pp. 354–362, 2018.

[12] N. Agah, B. Evans, X. Meng, and H. Xu, "A Local Machine Learning Approach for Fingerprint-based Indoor Localization," in *SoutheastCon 2023*, Apr. 2023, pp. 240–245, iSSN: 1558-058X. [Online]. Available: https://ieeexplore.ieee.org/document/10115169

[13] H.-X. Liu, B.-A. Chen, P.-H. Tseng, K.-T. Feng, and T.-S. Wang, "Map-Aware Indoor Area Estimation with Shortest Path Based on RSS Fingerprinting," in *2015 IEEE 81st Vehicular Technology Conference (VTC Spring)*, May 2015, pp. 1–5, iSSN: 1550-2252. [Online]. Available: https://ieeexplore.ieee.org/document/7145926

[14] O. Tasbaz, V. Moghtadaiee, and B. Farahani, *Zone-Based Federated Learning in Indoor Positioning*, Nov. 2022, pages: 168.

[15] N. Anzum, S. F. Afroze, and A. Rahman, "Zone-based indoor localization using neural networks: A view from a real testbed," in *2018 IEEE International Conference on Communications (ICC)*, 2018, pp. 1–7.

[16] M. Laska and J. Blankenbach, "Deeplocbim: Learning indoor area localization guided by digital building models," *IEEE Internet of Things Journal*, vol. 9, pp. 1–1, 08 2022.

[17] 5g tools, "5g nr timing advance distance calculator," accédé le : 27-09-2024. [Online]. Available: https://5g-tools.com/5g-nr-timing-advance-ta-distance-calculator/

[18] Y. Li, Z. Zhang, L. Wu, J. Dang, and P. Liu, "5g communication signal based localization with a single base station," in *2020 IEEE 92nd Vehicular Technology Conference (VTC2020-Fall)*, 2020, pp. 1–5.

[19] A. Le Floch, R. Kacimi, P. Druart, Y. Lefebvre, and A.-L. Beylot, "Accurate e-cid framework for indoor positioning in 5g using path tracing and machine learning," in *Proceedings of the Int'l ACM Conference on Modeling Analysis and Simulation of Wireless and Mobile Systems*, ser. MSWiM '23. New York, NY, USA: Association for Computing Machinery, 2023, p. 9–17.

[20] 3GPP, "3gpp tr 21.916," https://portal.3gpp.org/desktopmodules/Specifications/SpecificationDetails.aspx?specificationId=3493, accessed: 2023-12-04.

[21] A. Le Floch, R. Kacimi, P. Druart, Y. Lefebvre, and A.-L. Beylot, "A comprehensive framework for 5g indoor localization," *Computer Communications*, vol. 228, p. 107968, 2024. [Online]. Available: https://www.sciencedirect.com/science/article/pii/S0140366424003153

[22] A. Rai, K. K. Chintalapudi, V. N. Padmanabhan, and R. Sen, "Zee: zero-effort crowdsourcing for indoor localization," in *Proceedings of the 18th annual international conference on Mobile computing and networking*. Istanbul Turkey: ACM, Aug. 2012, pp. 293–304. [Online]. Available: https://dl.acm.org/doi/10.1145/2348543.2348580

[23] A. Le Floch, R. Kacimi, P. Druart, Y. Lefebvre, and A.-L. Beylot, "Indoor localization in current 5g networks: The way to go," in *2024 IFIP Networking Conference (IFIP Networking)*, 2024, pp. 285–293.